

Low-cost frequency-domain photon migration instrument for tissue spectroscopy, oximetry, and imaging

Yunsong Yang

University of Pennsylvania
Department of Biochemistry and Biophysics
Philadelphia, Pennsylvania 19104
E-mail: yunsong@eniach.upenn.edu

Hanli Liu, MEMBER SPIE

University of Texas at Arlington
Biomedical Engineering
PO Box 19138
Arlington, Texas 76019
E-mail: hanli@utarig.uta.edu

Xingde Li

University of Pennsylvania
Department of Physics
Philadelphia, Pennsylvania 19104
E-mail: xingde@sol1.lrsr.upenn.edu

Britton Chance

University of Pennsylvania
Department of Biochemistry and Biophysics
Philadelphia, Pennsylvania 19104
E-mail: chance@mail.med.upenn.edu

Abstract. We described a low-cost, frequency-domain photon migration spectroscopy instrument by using in-phase and quadrature demodulation technique in a 140-MHz homodyne system. A time constant of 1 ms was obtained. A frequency-division multiplexing technique was used for multiposition or multiwavelength applications, such as for tissue oximetry. By conducting several experiments on tissue/blood models, we show that the optical properties of tissue can be determined with this system by either using multiple source-detector separations at accuracy better than 8% or using single source-detector separation. The accuracy with the latter method can be improved to be 10% or better by choosing a proper calibration sample. A frequency-sweep system (30 to 700 MHz) was also implemented; the phase and amplitude measured on a tissue-like solution at 780 nm agreed to their theoretical values within 5% and 10% accuracy, respectively. © 1997 Society of Photo-Optical Instrumentation Engineers. [S0091-3286(97)03005-5]

Subject terms: photon migration; frequency-domain spectroscopy; in-phase and quadrature demodulation; frequency-division multiplex; absorption and scattering coefficients; noninvasive tissue oximetry.

Paper 26036 received March 18, 1996; revised manuscript received Oct. 1, 1996 and Dec. 13, 1996; accepted for publication Dec. 13, 1996.

1 Introduction

The determination of the optical properties of biological tissue is of primary importance in many fields in medicine for both diagnostics and monitoring. In the near-IR region (700 to 900 nm), the light absorption of typical tissue constituents, such as hemoglobin, exceeds that of water, providing a good spectral window for noninvasive tissue spectroscopy, oximetry, and imaging. Many techniques have been demonstrated in both the time domain and the frequency domain to obtain quantitative optical properties, namely, the absorption coefficient (μ_a) and the reduced scattering coefficient^{1,2} (μ'_s). While the time-resolved spectroscopy instrument has shown better sensitivity, the frequency-domain method can be achieved more economically and is more suitable for real-time monitoring in clinical usage. Several frequency-domain systems have been developed in different forms by measuring (1) only phase at one or two fixed frequencies,¹ (2) both phase and amplitude at fixed frequencies,² and (3) both phase and amplitude over a broad frequency range.³

Two modulation schemes exist in current frequency-domain spectroscopy instruments. One scheme can be classified as the heterodyne method, which uses one radio frequency (rf) for the test signal and another rf frequency for a reference signal. The phase and amplitude information generated at the test frequency are converted down to a low frequency by mixing the two rf signals and then detected by

a low-frequency phase meter and power meter. This method is basically the same technology as that used in the traditional amplitude modulation (am) radio technology. Another scheme can be called the single-sideband (SSB) method, which differs from the heterodyne method by generating a sideband signal as the second rf signal. Both schemes require a bandwidth ranging from a few hundred Hertz to several ten thousands of Hertz, and frequency stability and synchronization are critical. Moreover, in multiposition or multiwavelength applications, a time or frequency multiplex sharing technique can be employed to determine tissue optical properties, namely, absorption μ_a and reduced scattering μ'_s coefficients.⁴ To obtain a frequency scan, a network analyzer (Hewlett-Packard Model 8753C) can be used to implement the measurement over a wide frequency range.³ However, the cost of the analyzer is much higher than the other mentioned techniques.

In this paper, we describe a homodyne system that employs an available in-phase and quadrature demodulation circuit used in a novel way to determine the optical properties of tissue. We also use a unique frequency-division multiplexing system for dual wavelength detection. In addition, a low-cost broadband measurement system is implemented. Several experiments have been conducted to test the performance of each system, and the consistency between the experimental results and theoretical predictions confirms the significance and feasibility of the system.

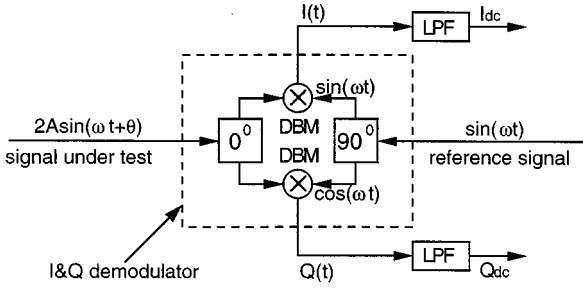


Fig. 1 Schematic diagram of an I&Q demodulator for detecting amplitude and phase of a rf signal.

2 Method

2.1 In-Phase and Quadrature Demodulation Technique

A standard in-phase and quadrature (I&Q) demodulator gives an I&Q signal within its working frequency range ω and detects both the ac amplitude A and the phase θ of a desired sinusoidal signal. Figure 1 shows that the standard I&Q demodulator consists of a pair of double-balanced mixers (DBMs) driven from a quadrature reference source, a 0-deg power splitter, and a 90-deg power splitter. One of the DBMs (i.e., the in-phase mixer) functions like a multiplier and produces an output $I(t)$ as

$$\begin{aligned} I(t) &= 2A \sin(\omega t + \theta) \sin(\omega t) \\ &= A \cos \theta - A \cos(2\omega t + \theta), \end{aligned} \quad (1)$$

and the other mixer (i.e., the quadrature mixer) produces an output $Q(t)$ as

$$\begin{aligned} Q(t) &= 2A \sin(\omega t + \theta) \cos(\omega t) \\ &= A \sin \theta + A \sin(2\omega t + \theta), \end{aligned} \quad (2)$$

where $A \sin \theta$ and $A \cos \theta$ are dc signals that carry the amplitude and phase information of the desired signal, and $A \sin(2\omega t + \theta)$ and $A \cos(2\omega t + \theta)$ are rf signals, which can be blocked by using low-pass filters (LPFs). Therefore, the phase and amplitude of the desired signal can be determined by

$$\theta = \tan^{-1} \left(\frac{Q_{dc}}{I_{dc}} \right), \quad (3)$$

$$A = (I_{dc}^2 + Q_{dc}^2)^{1/2}, \quad (4)$$

where $I_{dc} = A \cos \theta$ and $Q_{dc} = A \sin \theta$ are two dc outputs of the I&Q demodulator. The dc offset of the standard IQ circuit can be calibrated by measuring the background signal without the rf input and then subtracting it from I_{dc} and Q_{dc} .

Furthermore, since the outputs of I_{dc} and Q_{dc} are independent of the input frequency ω , a broadband I&Q demodulator can be utilized for frequency-sweep measurements. The bandwidth of such an instrument depends

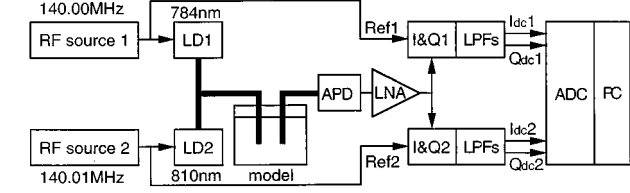


Fig. 2 Block diagram of a frequency-division multiplexing dual-wavelength optical detection system.

mainly on that of the demodulator. The outputs of the broadband instrument can be dc signals containing the phase and amplitude information provided LPFs can reject any frequency above the lowest frequency of the scanning range.

2.2 Frequency-Division Multiplexing System

Two rf signals with two slightly different frequencies ω_1 and ω_2 ($\omega_1 - \omega_2 = \Delta\omega \ll \omega_1$) can be expressed as $y_1 = 2A_1 \sin(\omega_1 t + \theta_1)$ and $y_2 = 2A_2 \sin(\omega_2 t + \theta_2)$, where θ_1 and θ_2 correspond to the phase shifts for signals y_1 and y_2 , respectively. If a narrow-band I&Q demodulator working at a center frequency of ω_1 is used to detect a superposed signal of y_1 and y_2 , the output of the demodulator in the $I(t)$ branch consists of four components as

$$\begin{aligned} I(t) &= [2A_1 \sin(\omega_1 t + \theta_1) + 2A_2 \sin(\omega_2 t + \theta_2)] \sin(\omega_1 t) \\ &= A_1 \cos(\theta_1) - A_1 \cos(2\omega_1 t + \theta_1) \\ &\quad + A_2 \cos[(\omega_1 - \omega_2)t + \theta_2] \\ &\quad - A_2 \cos[(\omega_1 + \omega_2)t + \theta_2]. \end{aligned} \quad (5)$$

Similarly, the output in the $Q(t)$ branch is

$$\begin{aligned} Q(t) &= [2A_1 \sin(\omega_1 t + \theta_1) \\ &\quad + 2A_2 \sin(\omega_2 t + \theta_2)] \cos(\omega_1 t) \\ &= A_1 \sin(\theta_1) + A_1 \sin(2\omega_1 t + \theta_1) + A_2 \\ &\quad \times \sin[(\omega_1 - \omega_2)t + \theta_2] + A_2 \sin[(\omega_1 + \omega_2)t + \theta_2]. \end{aligned} \quad (6)$$

By applying proper LPFs to the output of each branch (I and Q) of the demodulator, one can filter out the signals at frequencies of $2\omega_1$, $\omega_1 + \omega_2$, and $\omega_1 - \omega_2 = \Delta\omega$ and obtain only the dc components $A_1 \cos(\theta_1)$ and $A_1 \sin(\theta_1)$ for signal y_1 . If another narrow-band I&Q demodulator working at the frequency of ω_2 and corresponding LPFs are employed, we can also obtain the dc components $A_2 \cos(\theta_2)$ and $A_2 \sin(\theta_2)$ for signal y_2 . The choices of cut-off frequencies for LPFs depend mainly on the differential frequency of the two mixed signals $\Delta f = (\Delta\omega/2\pi)$.

2.3 Optical Instrument

A frequency-division multiplexing system can be used for dual-wavelength optical detection and is schematically illustrated in Fig. 2. Two low phase noise (-110 dBc/Hz at

10 kHz offset) rf signal generators operate at 140.00 and 140.01 MHz ($\Delta f = 10$ kHz) and provide the driving signals for two laser diodes (LDs) (Sharp LT022 and LT010, or LT024 and LT015 for higher power), which work at different optical wavelengths (e.g., 780 and 810 nm, or 780 and 830 nm). The rf signal generators also provide the reference signals at the corresponding frequencies for two narrow-band I&Q demodulators (Mini-circuits, MIQY-140D), respectively, with a bandwidth of 6 MHz. Typically, the I&Q demodulators have 0.15-dB amplitude unbalance and 0.5-deg phase unbalance. The two amplitude-modulated laser beams are combined and fiber coupled to the tissue model. The collected optical signal is fiber coupled to an avalanche photodiode (APD) with a diameter of 0.5 mm (Hamamatsu C5331). The electronic signal from the APD output (-100 to -60 dBm) is amplified by two low-noise amplifiers (LNA) (Mini-Circuits MAN-1LN) before being split into the I&Q demodulators.

For each I&Q demodulator, a pair of LPFs with a cutoff frequency of 160 Hz (equivalent to a time constant of 1 ms) and an attenuation rate of 30 dB/decade are built for the outputs of the I and Q branches to provide enough rejection for the 10-kHz differential frequency contained in the signal. As illustrated in Fig. 2, LD1 at wavelength 784 nm is encoded with 140.00 MHz, and thus the two dc outputs from the LPFs after demodulator I&Q1 will contain the amplitude and phase information only for the 784-nm signal. Similarly, the two dc outputs from I&Q2 after the LPFs give the information only for the 810-nm signal. Then the total four dc outputs are digitized in sequence by a PC-based, 12-bit, analog-to-digital converter (ADC) (Real-time Device AD2110) within 80 ms. Therefore, the desired I_{dc} and Q_{dc} signals for each wavelength can be separated without losing response time. And then the phases and amplitudes at two wavelengths can be calculated using Eqs. (3) and (4).

In addition, a single-wavelength, broadband system has been set up by switching the fixed-frequency source to a function generator (Rohde & Schwarz SMY 01) as a variable frequency source, the narrow-band APD to a wideband APD (Hamamatsu C5658) as the photon detector, and the narrow-band I&Q demodulator to a broadband I&Q demodulator. The broadband demodulator has a frequency range of 30 MHz to 1 GHz with 0.5-dB amplitude unbalance and 3-deg phase unbalance, typically.

2.4 Calibration and Quantification

The initial phase and amplitude due to the instrumental response need to be calibrated to quantify the measurements. While a slope protocol based on multiple source-detector separations has been demonstrated,² it is still inevitable to perform a calibration if different light sources or detectors are employed. Moreover, using multiple sources or detectors raises problems, such as prolonged measurement time and error caused by channel to channel delay. In this study, we employ a calibration procedure to quantify μ_a and μ_s' with single source-detector separation; this precalibration approach has been used to increase spatial resolution for near infrared imaging of tissue.⁵ Analytical expressions of ac amplitude and phase shift as functions of μ_a and μ_s' at a specific frequency under the infinite bound-

ary condition have been given by using the diffusion approximation.² After converting $\sin [(1/2) \tan^{-1} (\omega/v\mu_a)]$ to $[(\omega^2 + v^2\mu_a^2)^{1/2} - v\mu_a]/(\omega^2 + v^2\mu_a^2)^{1/4}$ based on trigonometry, we can express the phase shift θ_{measure} and amplitude A_{measure} as follows:

$$\theta_{\text{measure}} = \frac{r[(\omega^2 + v^2\mu_a^2)^{1/2} - v\mu_a]^{1/2}}{(2vD)^{1/2}} + \theta_0, \tag{7}$$

and

$$A_{\text{measure}} = \frac{A_0 \exp\{-r[(\omega^2 + v^2\mu_a^2)^{1/2} + v\mu_a]^{1/2}/(2vD)^{1/2}\}}{4\pi vDr}, \tag{8}$$

where θ_0 and A_0 are the initial phase and amplitude due to the instrumental response, r is the source-detector separation, $D = 1/(3\mu_s')$, ω is the modulation frequency, and v is the speed of light in the medium. Here θ_0 and A_0 can be calibrated by measuring a standard model with known μ_a and μ_s' . Then the following measurements for an unknown object can be quantified by

$$\theta_{\text{measure}} - \theta_0 = \frac{r[(\omega^2 + v^2\mu_a^2)^{1/2} - v\mu_a]^{1/2}}{(2vD)^{1/2}}, \tag{9}$$

and

$$\ln\left(\frac{A_{\text{measure}}}{A_0}\right) + \ln(4\pi vDr) = -\frac{r[(\omega^2 + v^2\mu_a^2)^{1/2} + v\mu_a]^{1/2}}{(2vD)^{1/2}}. \tag{10}$$

We notice that the product of Eqs. (9) and (10) yields

$$(\theta_{\text{measure}} - \theta_0) \left[\ln\left(\frac{A_{\text{measure}}}{A_0}\right) + \ln(4\pi vDr) \right] = -\frac{r^2\omega}{2vD}. \tag{11}$$

Therefore, D can be determined by iterating the following equation

$$D = -\frac{r^2\omega}{2v(\theta_{\text{measure}} - \theta_0) \left[\ln(A_{\text{measure}}/A_0) + \ln(4\pi vDr) \right]}, \tag{12}$$

and then μ_a can be calculated from either Eq. (7) or Eq. (8).

Tissue hemoglobin concentration and saturation can be calculated by solving the following linear equations⁶:

$$\mu_a^{780} = \epsilon_{\text{Hb}}^{780}[\text{Hb}] + \epsilon_{\text{HbO}_2}^{780}[\text{HbO}_2] + \mu_{a_b}^{780}, \tag{13}$$

$$\mu_a^{810} = \epsilon_{\text{Hb}}^{810}[\text{Hb}] + \epsilon_{\text{HbO}_2}^{810}[\text{HbO}_2] + \mu_{a_b}^{810}, \tag{14}$$

for [Hb] and [HbO₂], and then calculating

$$[\text{Hb}_{\text{total}}] = [\text{Hb}] + [\text{HbO}_2], \quad (15)$$

$$\text{saturation} = \frac{[\text{HbO}_2]}{[\text{Hb}_{\text{total}}]}, \quad (16)$$

where $\epsilon_{\text{Hb}}^{780}$, $\epsilon_{\text{HbO}_2}^{780}$, $\epsilon_{\text{Hb}}^{810}$, and $\epsilon_{\text{HbO}_2}^{810}$ are the extinction coefficients of deoxygenated and oxygenated hemoglobin at 780 and 810 nm, respectively, $[\text{Hb}]$ and $[\text{HbO}_2]$ are the concentrations of deoxygenated and oxygenated hemoglobin, $\mu_{a_b}^{780}$ and $\mu_{a_b}^{810}$ are the background absorption coefficients. Based on Ref. 7, we used $\epsilon_{\text{Hb}}^{780} = 0.626$, $\epsilon_{\text{HbO}_2}^{780} = 0.405$, $\epsilon_{\text{Hb}}^{810} = 0.453$, and $\epsilon_{\text{HbO}_2}^{810} = 0.513$ in units of $\text{mM}^{-1} \text{cm}^{-1}$ and assumed $\mu_{a_b}^{780} = \mu_{a_b}^{810}$. There exists a conversion factor of $\ln(10) = 2.3$ between our ϵ values and those given in Ref. 7. This factor stems from different definitions of the extinction coefficient ϵ and the absorption coefficient μ_a , which are defined as $I/I_0 = 10^{-\epsilon CL} = \exp(-\ln(10)\epsilon CL) = \exp(-\mu_a L)$, where I and I_0 are the detected and incident light intensity of an optical signal passing through an absorbing medium, C is the absorber concentration, and L is the optical mean pathlength traveled by light in the medium. We are aware that the wavelength pair of 780 to 810 nm is not the optimum choice for its sensitivity in determining hemoglobin saturation.¹ However, a theoretical calculation shows that when the saturation value decreases from 100 to 0%, the ratio of $\mu_a(780)/\mu_a(810)$ will change from 0.8 to 1.4, whereas the ratio of $\mu_a(754)/\mu_a(810)$ will change from 0.65 to 1.9. This means that using the 780- to 810-nm wavelength pair is about 50% as sensitive as using 754- to 810-nm pair to detect changes in hemoglobin saturation. The advantage of using 780- and 810-nm wavelengths is to expect an equal but opposite response at these two wavelengths when the level of hemoglobin saturation is changed. This is because the differences between the extinction coefficients of the oxygenated and deoxygenated hemoglobin at these two wavelengths are about the same but with reverse signs at each side of the isosbestic point ($=800$ nm).

3 Experiments and Results

The accuracy of a frequency-domain instrument in determining optical properties can be influenced by not only the precision of the instrument itself but also the physical algorithm to extract values of μ_a and μ'_s . In this section, we first use the well-established slope (multiseparation) protocol to study the accuracy of the I&Q instrument and then use the calibration single-separation procedure to compare the accuracy between these two methods. Experimental results on blood oxygenation tests are also given to demonstrate the accuracy of the system in the determination of hemoglobin saturation. Finally, we show a good consistency between theoretical predictions and the experimental data measured with our broadband I&Q system at multiple frequencies.

The slope protocol measurement was conducted to compare our system with other apparatuses. The setup shown in Fig. 2 was used with precision of 0.5 mV in amplitude and of 0.5 deg in phase. A stepping-motor-controlled mechanical holder was utilized to provide different source-detector

separations in a moving range of 2 to 6 cm with an interval of 0.5 cm. Within the linearity of the system, six source-detector separations were chosen for the slope calculation, and the choices of the separations depend on both the Intralipid and ink concentrations of the sample solutions. The optical properties were calculated in the same way as described by Fishkin and Gratton.² Figures 3(a), 3(b), 3(c), and 3(d) show the results of μ_a and μ'_s for a 40-l Intralipid solution. In the case of Figs. 3(a) and 3(b), there was no ink in the solution, the concentrations of Intralipid for the three measurements were 0.48, 0.53, and 0.58% to obtain different μ'_s values. These two figures show that μ'_s values are linear with the Intralipid concentration for both wavelengths, and μ_a values remain constant. In the case of Figs. 3(c) and 3(d), the Intralipid concentration was kept 0.6%, while the concentration of ink was varied to obtain different μ_a values. The μ_a values in these two graphs are linear with the ink concentration, while the μ'_s values hold constant. These results are consistent with the theory and those measured using the time-domain method. The accuracy in determining μ_a values is better than 5% based on Ref. 8 and the corresponding spectrophotometer measurements, and the accuracy for μ'_s values is better than 8% in comparison to other frequency-domain equipment.⁹ Therefore, the I&Q demodulation technique with the slope algorithm can be used to quantify the optical properties of tissue with accuracy better than 8%.

Based on Eqs. (7) and (12), we also employed the single source-detector separation algorithm with a calibration procedure to calculate μ_a and μ'_s . Figures 4(a) and 4(b) show comparisons of μ_a and μ'_s values, respectively, obtained using the slope and single source-detector separation methods for the same data as given in Figs. 3(a) and 3(b) at 780 nm. The two dashed traces in Figs. 4(a) and 4(b) are obtained with the calibration algorithm at 3 and 4 cm for two individual source-detector separations. The initial 0.487% Intralipid solution was used as the calibration sample. The maximum deviations between the values obtained with the two methods at 0.54 and 0.58% Intralipid concentrations are less than 2% for both μ_a and μ'_s . In addition, Figs. 4(c) and 4(d) plot the μ_a and μ'_s dependency, respectively, of a 16-l, Intralipid-ink solution on the ink concentration at 780 nm. The data in these two figures were calculated using the slope and single-separation methods. The solution with the lowest ink concentration was taken as the calibration medium. The two individual source-detector separations used in the single source-detector separation calculations were 4 and 4.5 cm. It is seen that the deviation due to the two algorithms becomes larger (up to 25%) as the absorption difference between the calibration and unknown sample increases from 0 to 0.12 cm^{-1} . This is consistent with theoretical simulations given for a continuous wave system,¹⁰ which is a special case of a frequency-domain system ($f=0$). The results at 830 nm are very similar to those at 780 nm given in Figs. 4(a) to 4(d). Therefore, we suggest that the accuracy of the single source-detector separation method will increase as the difference of optical properties between the calibration and the unknown medium decreases, particularly, as the absorption properties of the two media become similar. For example, if the absorption co-

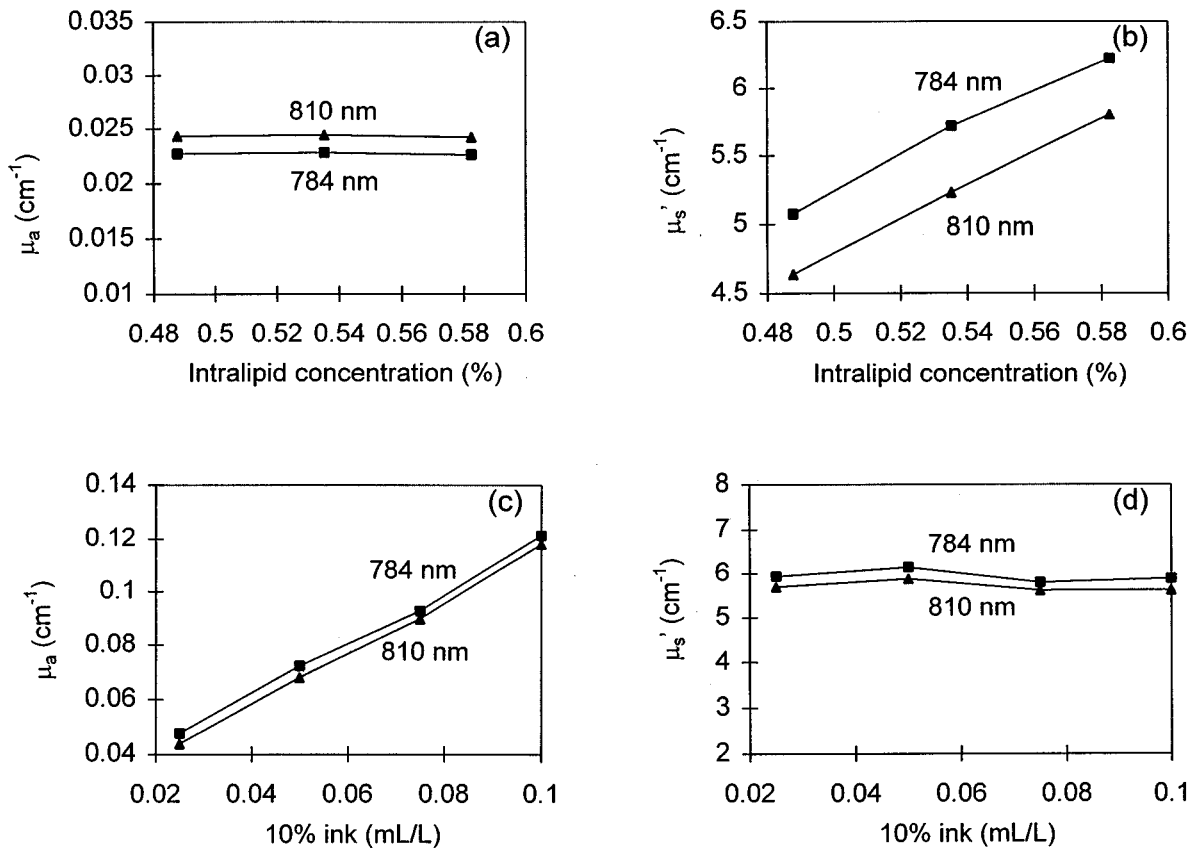


Fig. 3 Experimental results of μ_a and μ_s' of a 40-l Intralipid solution measured at 784 nm (squares) and 810 nm (triangles) with the frequency-division multiplexing dual wavelength instrument and calculated with the slope protocol. In (a) and (b), there was no ink in the solution, and the concentration of Intralipid was varied to obtain different μ_s' values. In (c) and (d), the Intralipid concentration was kept 0.6%, and the concentration of ink was varied to obtain different μ_a values.

efficient of a sample varies from 0.04 to 0.1 cm^{-1} , which is a typical range for most of tissues, the accuracy of the I&Q system with the single source-detector separation method can be improved by choosing the μ_a value of the calibration sample to be 0.07 cm^{-1} .

Experiments on blood oxygenation and deoxygenation tests were conducted with the frequency-division multiplexing, dual-wavelength instrument with single source-detector separation. The scattering medium consisted of a 1-l, 0.5% Intralipid solution with yeast added into the solution to consume oxygen via respiration. We repeatedly added 2 ml of whole rat blood into the solution after each deoxygenation cycle. After the addition of blood, 99.9% oxygen gas was supplied to the solution until a P_{O_2} (oxygen pressure) monitor indicates a full-saturation condition. The quantitative values of μ_a and μ_s' were obtained based on Eqs. (7) and (12), and the initial solution without any blood was used as the calibration sample. Hemoglobin concentration and saturation were calculated after the subtraction of background absorption, namely, water absorption with values⁹ of $\mu_{a_b}(784 \text{ nm}) = \mu_{a_b}(810 \text{ nm}) = 0.023 \text{ cm}^{-1}$. Figure 5(a) shows that the hemoglobin concentration increases linearly with the addition of blood. The actual hemoglobin concentration can also be calculated by

$$\frac{\text{volume of whole rat blood}}{\text{total volume of the solution}} \times 8 \text{ mM}, \tag{17}$$

assuming that the hemoglobin concentration of whole blood is 8 mM (Ref. 6). The deviations of the hemoglobin concentrations obtained using the experimental data [Fig. 5(a)] from the actual values calculated using Eq. (17) are less than 5%. Figure 5(b) illustrates that the saturation values swing between 0 and 90% during oxygenating and deoxygenating processes. The absolute errors of the saturation determination in the higher end and lower end are about 15 and 10%, respectively. Although these errors seem nontrivial, so far no other existing near-IR frequency-domain equipment can give better results than these values for blood/tissue model tests. Figure 5(c) shows that the reduced scattering coefficients μ_s' at both 784 and 810 nm remain relatively constant, with a deviation less than 2%, when the blood concentration and thus the absorption of the solution increases during five cycles of the experiment. Thus, tissue spectroscopy and oximetry can be achieved using the narrow-band I&Q system with accuracy of 5% for scattering properties and hemoglobin concentrations and with an absolute error of 10 to 15% for hemoglobin

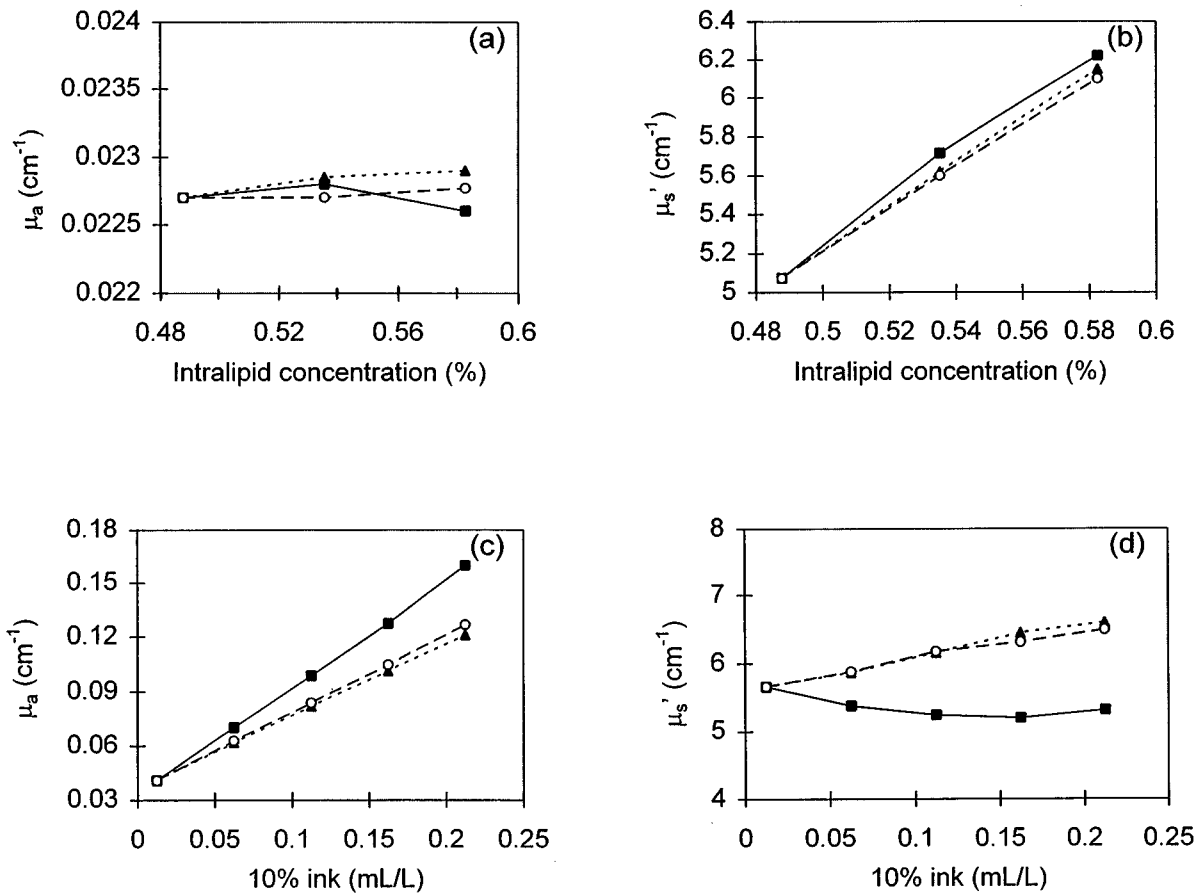


Fig. 4 (a) and (b) Experimental results of μ_a and μ_s' of a 40-l, ink-free Intralipid solution calculated with the slope method (squares) and single source-detector separation method with $\rho=3$ cm (triangles) and $\rho=4$ cm (open circles). (c) and (d) Experimental results of μ_a and μ_s' of a 16-l, Intralipid-ink solution calculated with the slope method (squares) and single source-detector separation method with $\rho=4$ cm (triangles) and $\rho=4.5$ cm (open circles).

saturation. Further studies are needed to understand the cause of large errors in hemoglobin saturation.

In addition, we employed a frequency-sweep system, as described in earlier sections, to conduct a broadband measurement of optical properties of a 5-l, 0.5% Intralipid solution at multiple modulation frequencies. The measurements were scanned from 50 to 700 MHz with source-detector separations varying from 2 to 6 cm. The wavelength used in this case was 780 nm. The symbols plotted in Figs. 6(a) and 6(b) show the experimental results of amplitude and phase versus the source-detector separation at modulation frequencies of 100, 300, and 500 MHz. In addition, the solid lines plotted in both of the figures were obtained using the diffusion equation for an infinite medium with values of $\mu_a=0.03 \text{ cm}^{-1}$ and $\mu_s'=4.4 \text{ cm}^{-1}$ at the three corresponding frequencies. For a 0.5% Intralipid solution, this set of μ_a and μ_s' values are expected based on literature⁸ and the results obtained with other frequency-domain instruments.⁹ The consistencies between the experimental data and theory at other frequencies have also been observed (but not shown). In Fig. 6(a), some disagreement between the experimental data and theoretical calculation appears when the separation is smaller

than 2.5 cm. This inconsistency can be attributed to the photodetector saturation caused by the source and detector being too close and so having too strong light intensity. When the system works in its linear region, the experimental results are in a good agreement with the theoretical predictions at accuracy better than 5% for phase and 10% for amplitude. Therefore, these two figures demonstrate that the broadband I&Q system can provide accurate measurements for μ_a and μ_s' .

4 Discussion and Summary

To be suitable for clinical usage, a medical instrument must accomplish the performance required, such as accuracy, stability, and speed, as well as keep the cost of manufacturing, operation, and maintenance as low as possible. In this paper, we present an I&Q system that uses the I&Q demodulation technique to obtain the quantitative measurements of optical properties of tissue. As shown in precedent sections, the system can provide better than 8% accuracy for μ_a and μ_s' determinations with the slope algorithm and 10% accuracy with single source-detector separation by choosing an appropriate calibration sample. In addition, our

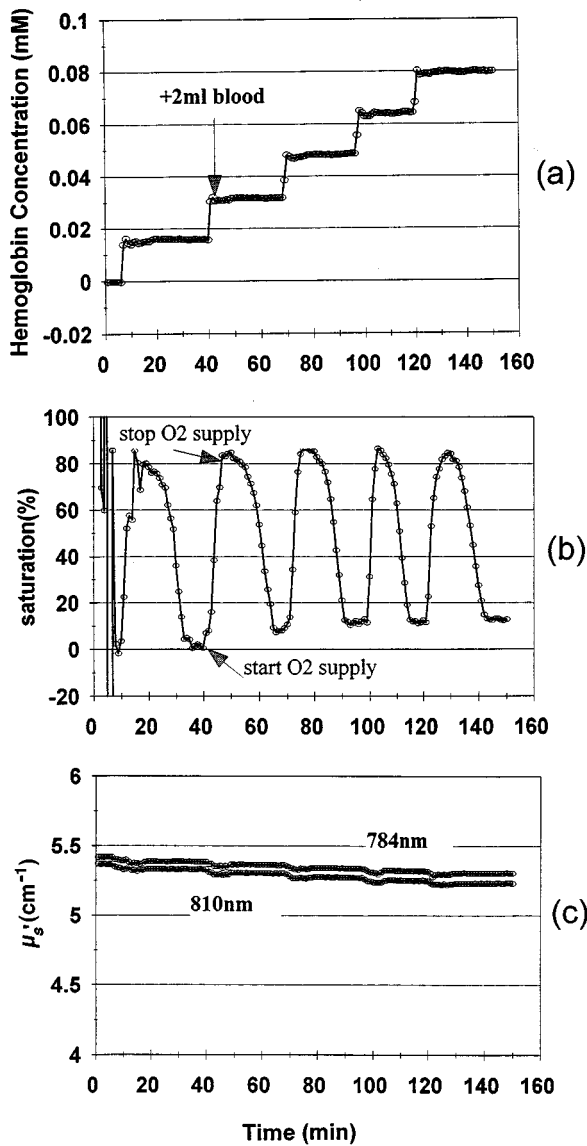


Fig. 5 Experimental results measured on blood oxygenation and deoxygenation tests by using frequency-division multiplexing dual wavelength instrument and single source-detector separation. We repeatedly added 2 ml of rat blood into a 1-l, 0.5% Intralipid solution. A certain amount of oxygen gas was supplied each time and then was consumed by yeast, which were already in the solution.

stability tests show that the amplitude and phase drift of the system are 0.5 dB and 1 deg, respectively, over 12 h. Since the time constant of the system is 1 ms, the system is capable of detecting fast signals varying in tens of milliseconds. To have a better SNR, the fast response time also enables us to acquire data within 80 ms/cycle of the four sequent outputs from the two I&Q demodulators. Therefore, it has a significant potential for real-time monitoring. Furthermore, as a common device used in telecommunication, standard I&Q demodulators are readily accessible and affordable. To build a narrow-band frequency-domain instrument, although using a functional generator or synthesizer with a high-speed ADC may not be considered expensive, a narrow-band I&Q system can even reduce the cost by a factor of 5 up to 10. Similarly, use of a broadband

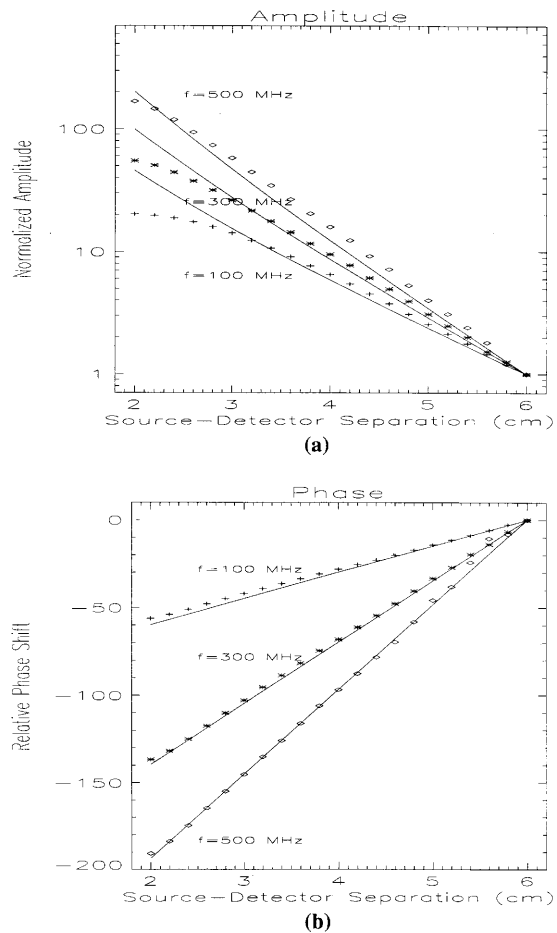


Fig. 6 Experimental results (symbols) and theoretical calculations (solid lines) of (a) amplitude and (b) phase dependence on source-detector separations at multiple modulation frequencies of 100, 300, and 500 MHz. The wavelength used for the measurements was 780 nm.

I&Q frequency-domain system will avoid employing the expensive network analyzer, and thus bring the cost down significantly, leading to a high performance-to-price ratio.

We have also demonstrated a frequency-division multiplexing technique for multichannel or multiwavelength applications. Using this technique, the measurement time can be shortened significantly, and it will be very advantageous for imaging applications. The errors caused by channel-to-channel delay in the case of time sharing could also be reduced. In addition, the principle we have described here can be easily adapted to applications in other fields, such as in chemical, food, and pharmaceutical industries, by choosing appropriate optical wavelengths and modulation frequencies. In summary, because of the simplicity, low cost, and readiness, the frequency-division multiplex technique utilizing I&Q demodulators shows a great potential to be commercialized in the fields of medicine and other industries in the near future.

Acknowledgments

The authors wish to thank Kenneth A. Simons for his valuable advice on instrumentation. They are also grateful to Maureen O’leary, Yutao Zhang, and Yong Wang for their

help. This work was supported in part by National Institutes of Health grants NS27346-04, CA60182-03, and CA50766-03.

References

1. E. M. Sevick, B. Chance, J. Leigh, S. Nioka, and M. Maris, "Quantitation of time- and frequency-resolved optical spectra for the determination of tissue oxygenation," *Anal. Biochem.* **195**, 330–351 (1991).
2. J. B. Fishkin and E. Gratton, "Propagation of photon-density waves in strongly scattering media containing an absorbing semi-infinite plane bounded by a straight edge," *J. Opt. Soc. Am. A* **10**, 127–140 (1993).
3. S. J. Madsen, E. R. Anderson, R. C. Haskell, and B. J. Tromberg, "Portable, high-bandwidth frequency-domain photon migration instrument for tissue spectroscopy," *Opt. Lett.* **19**(23), 1934–1936 (1994).
4. B. Chance, "Phase measurement of absorbers/scatters in human tissue," in preparation for publication.
5. M. A. Franceschini, S. Fantini, S. A. Walker, J. S. Maier, W. W. Mantulin, and E. Gratton, "Multichannel optical instrument for near-infrared imaging of tissue," *Proc. SPIE* **2389**, 264–273 (1995).
6. H. Liu, B. Chance, A. H. Hielscher, S. L. Jacques, and F. K. Tittel, "Influence of blood vessels on the measurement of hemoglobin oxygenation as determined by time-resolved reflectance spectroscopy," *Med. Phys.* **22**(8), 1209–1217 (1995).
7. W. G. Zijlstra, A. Buursma, and W. P. Meeuwssen-van der Roest, "Absorption spectra of human fetal and adult oxyhemoglobin, deoxyhemoglobin, carboxyhemoglobin, and methemoglobin," *Clin. Chem.* **37**, 1633–1638 (1991).
8. G. M. Hale and M. R. Querry, "Optical constants of water in the 200-nm to 200- μ m wavelength region," *Appl. Opt.* **12**(3), 555–563 (1973).
9. M. A. O'Leary and D. A. Boas, Univ. of Pennsylvania, Private Communication, 1995.
10. H. Liu, D. A. Boas, Y. Zhang, A. G. Yodh, and B. Chance, "A simple approach to characterize optical properties and blood oxygenation in tissue using continuous near infrared light," *Phys. Biol. Med.* **40**, 1983–1993 (1995).

Yunsong Yang received his BS in electrical engineering from Harbin Institute of Technology, China, in 1992. He is currently enrolled in the MS program in the Department of Electrical Engineering Department of the University of Pennsylvania. His research interests include biomedical instrumentation, noninvasive measurement, and IR tomography.

Hanli Liu graduated from Wake Forest University, North Carolina, and received her MS and PhD degrees in physics in 1990 and 1994, respectively. From June 1992 to August 1996, she was a research associate in the Department of Biochemistry and Biophysics at the University of Pennsylvania. She is currently an assistant professor in the Biomedical Engineering Department of the University of Texas at Arlington. Her scientific interests have been quantification of tissue optical properties and oxygenation, development of algorithms for evaluating light scattering and absorption changes in cells and tissues, and tumor detection by time-domain and frequency-domain spectroscopy using the near-IR light. She is a member of SPIE and is the author of more than 20 scientific papers.

Xingde Li received his BS from the University of Science and Technology of China in 1990 and has been a PhD candidate in physics and biophysics at the University of Pennsylvania working with Dr. Britton Chance and Dr. Arjun G. Yodh since 1992. His current projects are the fundamental theories and instrumentation in biomedical diagnosis and functional imaging using near-IR laser and fiber electro-optics and the light amplification effect in random media.

Britton Chance is Eldridge Reeves Johnson University Professor of Biophysics, Physical Chemistry, and Radiology at the University of Pennsylvania and received his BS and MS degrees from the University of Pennsylvania in 1935 and 1936, respectively, and PhD and DSc degrees from both the University of Pennsylvania and the University of Cambridge, in 1940 and 1951, respectively. He is a member of the National Academy of Sciences and of the Institute of Medicine and is a foreign member of the Royal Society of London. Among many other recognitions, he received the National Medal of Science, the Benjamin Franklin Medal from the American Philosophical Society, the Biological Physics Prize from the American Physical Society, and honorary degrees from the Karolinska Institute, the Medical College of Ohio at Toledo, Semmelweis University, Hahnemann Medical College, and the universities of Pennsylvania, Helsinki, Dusseldorf, and Buenos Aires.